# Propylene Polymerization in a Semibatch Slurry Reactor over Supported $TiCl_4$ / $MgCl_2$ / Ethyl Benzoate / Triethyl Aluminum Catalyst. II. A Kinetic Study Based on a Multisite Model

CONSTANTINE DUMAS* and CHENG C. HSU, *Chemical Engineering Department, Queen's University, Kingston, Ontario K7L 3N6, Canada*

## Synopsis

In propylene polymerization over $TiCl_4/MgCl_2$/ethyl benzoate (EB)/triethyl aluminum (TEA) catalysts, experimental evidence strongly suggests that active sites have differing propagation and termination rate constants. Although the chemical structure of these sites may be quite similar, their location on the support may affect their polymerization activity, and this results in a distribution of the propagation and deactivation rate constants. To model this type of system, we developed a kinetic model accounting for multiple active sites. The model was fitted to simulated polymerization data to investigate the validity of mathematical approximations used in the derivation of the model equation. Using experimental data, the adequacy of the model was tested, and the statistical inference of parameter estimation was also discussed. The effects of experimental operating variables and additives on the kinetic model parameters revealed an important insight into the fundamentals of this system. The optimum productivity commonly observed has been shown to be the result of differing rates of increase of both propagation and termination rates with Al/Ti ratio and temperature. Kinetic evidence also suggests that the additive selectively poisons atactic-specific sites.

## INTRODUCTION

Many attempts have been made to model propylene polymerization over supported catalyst of transition metal. However, the efforts appear to be not very successful. So far no single kinetic model in the literature can adequately describe the conversion behavior of the system over a wide range of polymerization conditions. Mechanistic models assuming active sites of uniform activity (single site) have been shown only applicable to the very early stage of polymerization. Some success has been achieved however by Keii et al.,[1] who have incorporated adsorption isotherms into a single-site model. Attempts at using empirical models have not been successful either. For instance, Brockmeier and Rogan[2] modeled the rate decay as a power law function of instantaneous polymerization rate and found that the order changed as a function of polymerization time.

*Present address: Engineering Research Laboratory, Central Research, Dow Chemical Company, Midland, MI 48640.

Journal of Applied Polymer Science, Vol. 37, 1625–1644 (1989)
 CCC 0021-8995/89/061625-20$04.00

Perhaps the main reason for the inadequacy of these models is the unrealistic assumption of uniform activity. As discussed previously by Dumas and Hsu,[3] it is likely that active sites have different polymerization and termination characteristics. It is conceivable that the difference in activity could result from the physical location of an active site on the support. The support not only acts as a physical dispersant of the sites, but actually reacts chemically with organo-complexes to form active sites. Therefore, depending on whether an active site is located on a crystal edge, face, or corner of either cubic close-packing, hexagonal close-packing, or rotationally disordered $MgCl_2$, the inductive effect of the chlorine atoms in $McCl_2$ may vary. This in turn affects the stability of the monomer-transition metal bond, and hence the polymerization activity of an active site. The physical location may also affect the steric environment of a site. Therefore, it is reasonable to assume that the propagation and termination rate constants vary from site to site, which can result in a broad distribution of site activity.

In this work we propose a multisite model to account for the possible existence of a large number of sites of different activities. The adequacy of the model will be examined using the kinetic data of propylene polymerization over $MgCl_2$ supported catalyst of $TiCl_4$/ethyl benzoate (EB)/triethyl aluminum (TEA).

## Development of Multisite Model

Assuming first-order propagation with respect to monomer, as has been generally accepted for coordination polymerization, the rate of polymerization for a multisite system based on total volume of the reaction mixture $V$ for a multisite system may be written as

$$R_p = \sum k_{pi}[C_i^*][M]V \tag{1}$$

where [M] is the monomer concentration, $[C_i^*]$ the concentration of active sites at the $i$th activity level, $k_{pi}$ the propagation rate constant of site $i$, and the summation is over all sites.

Catalyst deactivation may be a result of active site destruction, and sites of different activity may not decay at the same rate. It is important at this point in the development to briefly consider some of the possible mechanisms of active site decay.

Chien and Wu[4] have recently found that, with their catalytic system, some of the titanium on the catalyst surface is EPR (Electron paramagnetic resonance) silent, and they concluded that these atoms are therefore arranged in close proximity. They went on to speculate that some of the catalytic deactivation may occur by a second-order bimolecular reaction between adjacent active sites. In a subsequent modeling study, Chien and Kuo[5] used a single species model to show that second-order termination was plausible at very high Al/Ti ratios (Al/Ti $\geq$ 167); but, at more moderate Al/Ti ratios (Al/Ti = 42), first-order termination with respect to the concentration of active sites was indicated.

It is also possible that the organometallic complex, upon activation with alkyl aluminum, may be inherently unstable and may deactivate by a first-

order mechanism. It is also possible that various components in the bulk solution (e.g., moisture, additives, excess aluminum alkyl, or aluminum alkyl reaction byproducts) may react with and therefore deactivate the sites. If this were the case, the deactivation rate constant $k_{ti}$ would then be expected to vary with aluminum alkyl or electron donor additive concentration.

In this derivation, a first-order deactivation of sites was assumed:

$$d[\mathrm{C}_i^*]/dt = -k_{ti}[\mathrm{C}_i^*] \tag{2}$$

Because $k_{pi}$'s are assumed constant,

$$d\left(k_{pi}[\mathrm{C}_i^*]\right)/dt = -k_{ti}k_{pi}[\mathrm{C}_i^*] \tag{3}$$

To simplify the notation, we define

$$[\mathrm{C}_i'] = k_{pi}[\mathrm{C}_i^*] \qquad \text{and} \qquad \mathrm{C}' = \sum[\mathrm{C}_i']$$

so that eq. (3) now becomes,

$$d\mathrm{C}'/dt = -\sum k_{ti}[\mathrm{C}_i'] \tag{4}$$

and

$$d\mathrm{C}'/dt = -\mathrm{C}'\sum\left(k_{ti}[\mathrm{C}_i']/\mathrm{C}'\right) \tag{5}$$

Defining at $t = 0$,

$$k_{t0} = \sum k_{ti}[\mathrm{C}_i'](0)/\mathrm{C}'(0) \tag{6}$$

we can write eq. (5) in the following form:

$$d\mathrm{C}'/dt = -k_{t0}\mathrm{C}'\sum\left\{\left(k_{ti}[\mathrm{C}_i']/\mathrm{C}'\right)/k_{t0}\right\} \tag{7}$$

Kemp and Wojciechowski,[6] in their modeling of the catalytic cracking of mixed gas oil, which is also characterized by a large number of first-order parallel reactions, applied an approximation to eliminate the summation term. Applying the same approximation to eq. (7), we obtain

$$R_p = [\mathrm{M}]\mathrm{C}'(0)/\left\{(1 + k_{t0}\theta_3 t)^{1/\theta_3}\right\}V \tag{8}$$

where $\theta_3$ is a constant which must determined by kinetic data. Rearranging this equation, for use with the semibatch reactor system described in Part I of this series[7] results in

$$R_p/[\mathrm{M}] = \theta_1/\left\{(1 + \theta_2\theta_3 t)^{1/\theta_3}\right\} \tag{9}$$

where $\theta_1$ and $\theta_2$ are defined as

$$\theta_1 = V\sum k_{pi}[\mathrm{C}_i^*], \qquad \text{at } t = 0 \tag{10}$$

and

$$\theta_2 = \sum k_{ti} k_{pi} [C_i^*] / \sum k_{pi} [C_i^*], \qquad \text{at } t = 0 \tag{11}$$

With these definitions of $\theta$'s, we see that $\theta_1$ reflects the catalyst activity, whereas $\theta_2$ can be considered as the average termination rate constant weighted by the site activity. In the subsequent simulation study, it was indicated that $\theta_3$ can be considered as a dispersion parameter characterizing the distribution of active sites.

## Multisite Model Simulations

To examine the validity of the mathematical approximation of Kemp and Wojciechowski[6] used to obtain eq. (8), a series of model simulations were

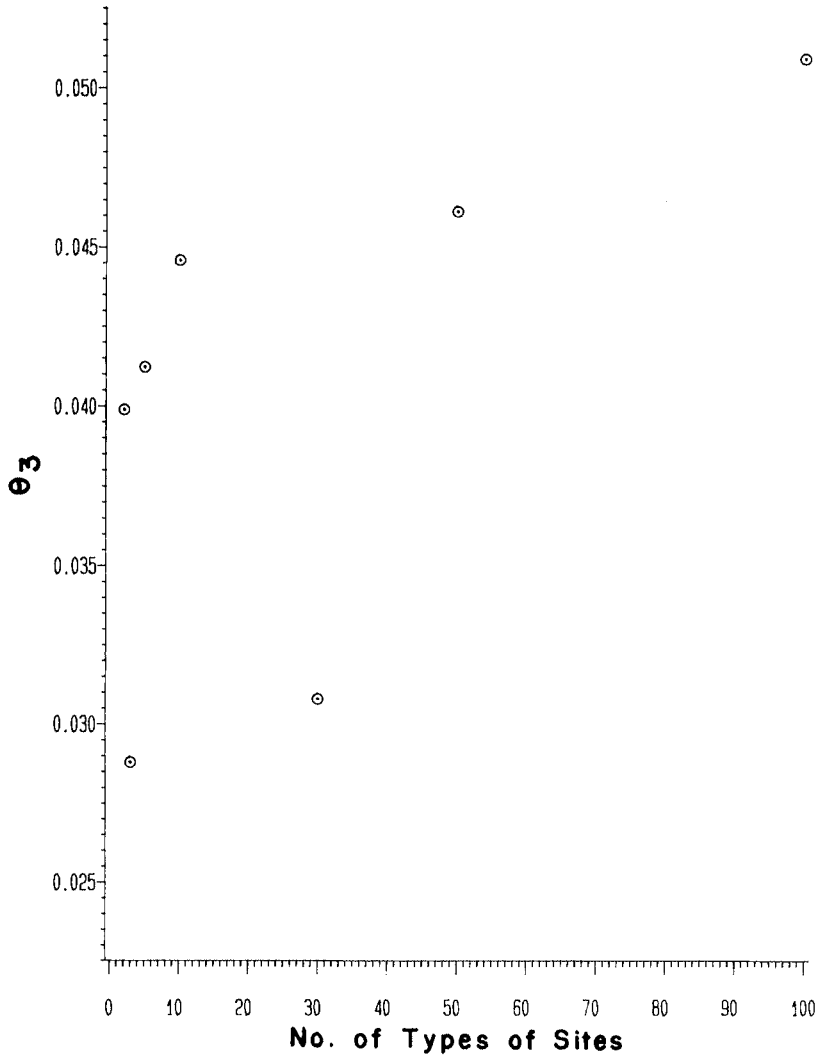


Fig. 1. Effect of the number of types of sites on $\theta_3$. Mean $k_t = 0.25$ with minimum $k_t = 0.24$, actual $\theta_1 = 1000$.

carried out, whereby the numerical values of $k_{pi}[C_i^*]$ ranging from 0 to 2000 and $k_{ti}$ from 0.24 to 0.26, based on an assumed distribution of active sites were assigned; then a simulated polymerization curve was generated using eq. (1). Because experimental evidence has suggested that sites with relatively high activities also decay relatively quickly (Doi et al.[8] and Giannini[9]), active sites with higher activities were assigned higher termination rate constants. The multisite model [eq. (9)] was subsequently fitted to this simulated data to obtain parameter estimates for $\theta_1$, $\theta_2$, and $\theta_3$ using a nonlinear least-squares curve fitting program "NOTLIN," from Queen's University computing library.

The estimated value of $\theta_1$, obtained by curve-fitting eq. (9) to the simulated polymerization curve, was 1014 compared to the true value of 1000. Similarly, the estimated value of $\theta_2$ was 0.266 compared to the true value of 0.254. These estimates deviate from the true values less than 5%.

Although a great deal of information suggests the possible existence of multiple active sites, the exact number of types of sites is not known. Therefore, to assess the performance of the multisite model for possible

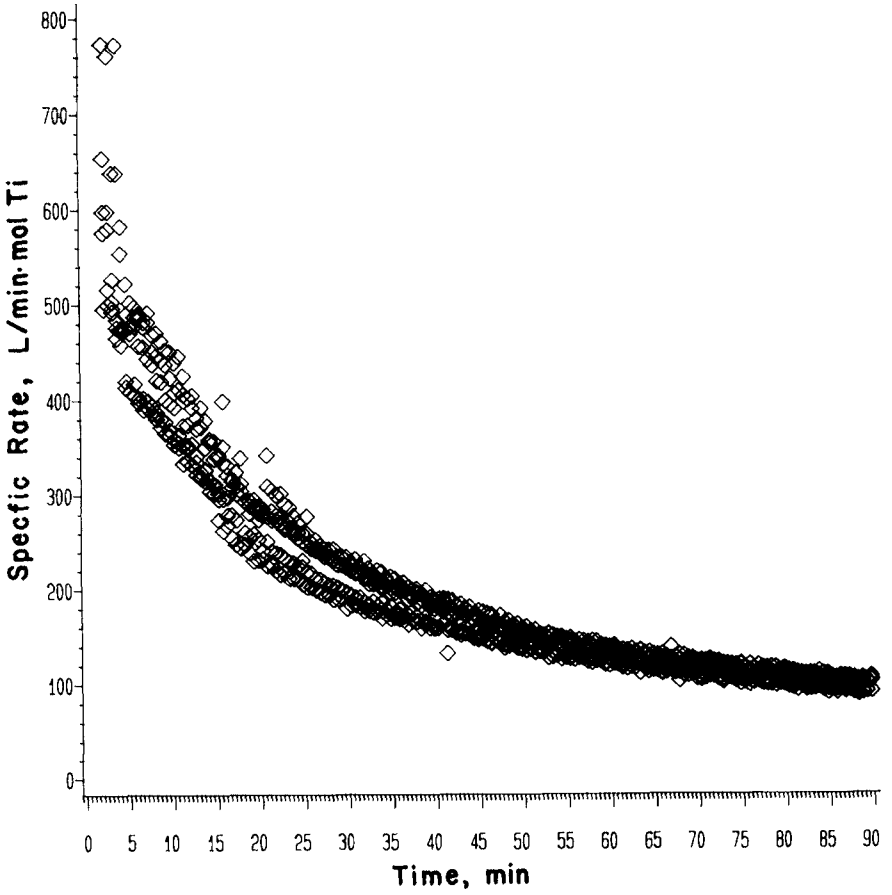


Fig. 2. Specific rate (referred to a reaction mixture volume of 0.23 L) curve for five replicate runs. Conditions: 50°C, [Ti] = 68.6 μmol/L, Al/Ti = 21.

extremes in the number of types of sites, a series of simulations were carried out using as few as two and as many as 100 types of active sites. Even with as few as two types of sites, the $\theta_1$ estimate is within 1.5% of the true value. Under the same condition, the $\theta_2$ estimate is within 4% of the true value.

It is also important to observe qualitatively the effect of the number of types of sites on the heterogeneity parameter $\theta_3$. As shown in Figure 1, $\theta_3$ increases as the number of types of sites increases.

In summary, it may be concluded from the simulation results that: (i) the parameter estimates for $\theta_1$ and $\theta_2$ of the multisite model eq. (9) closely approximated the mechanistic lumped parameters $\Sigma k_{pi}[C_i^*]$ and $\Sigma k_{ti}k_{pi}[C_i^*]/\Sigma k_{pi}[C_i^*]$, respectively, under a variety of simulation conditions; (ii) $\theta_2$ is directly proportional to the mean value of $k_{ti}$ and is relatively insensitive to changes in the mean value of $\theta_1$, as long as the distribution of activities

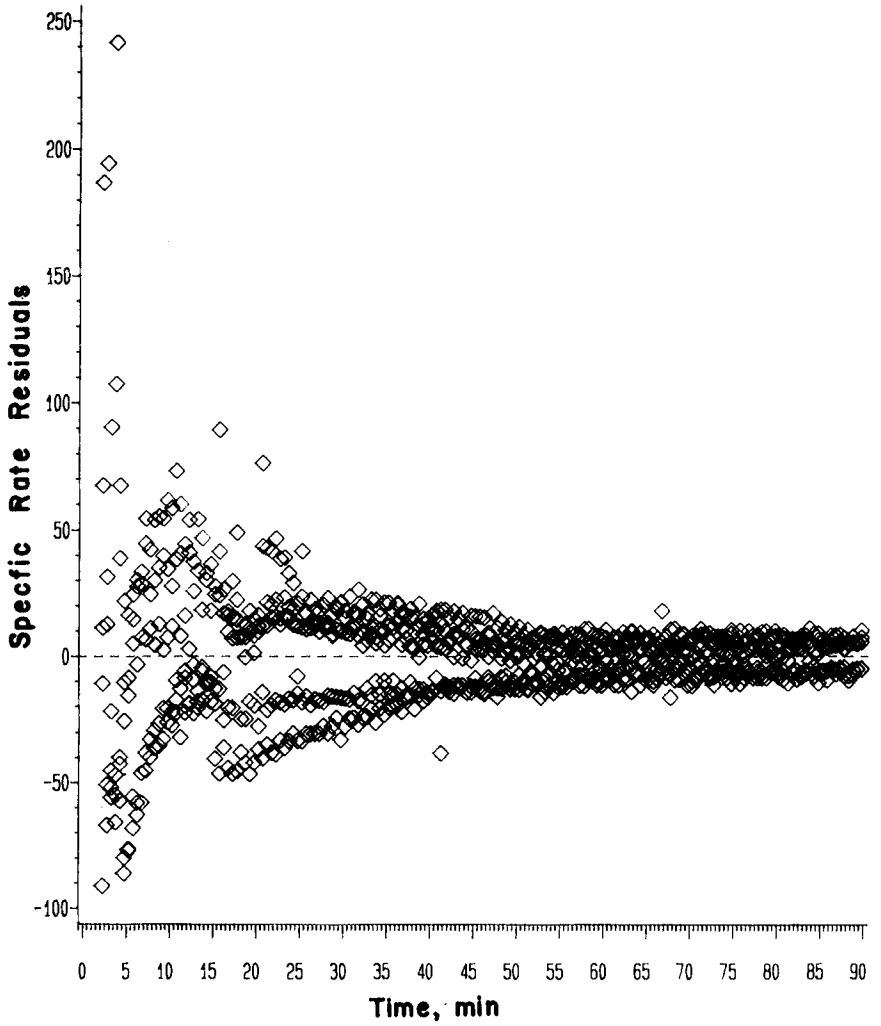


Fig. 3. Unweighted residuals from fitting the multisite model to the specific rate (1/mol min) data of five replicate runs.

remains the same; and (iii) the empirical power law parameter $\theta_3$ decreases as the distribution of activities and termination rates become homogeneous, and the number of types of active sites becomes small.

## RESULTS AND DISCUSSION

### Adequacy of the Multisite Model

In order to examine the model adequacy and error variance, five replicate experimental runs were performed using the experimental procedure discussed in Part I at 50 °C and Al/Ti = 20 (Dumas and Hsu[7]). Each run lasted 90 min, and the instantaneous rate of polymerization was computed for every 30 s of polymerization time. The multisite model was fitted to the data from these runs. A total of eight replicate runs were carried out; three of which were discarded because of apparent contamination. The results after mass transfer corrections are shown in Figure 2 where the specific rate, defined as $R_p$/[M] per mole of Ti, are plotted against time.

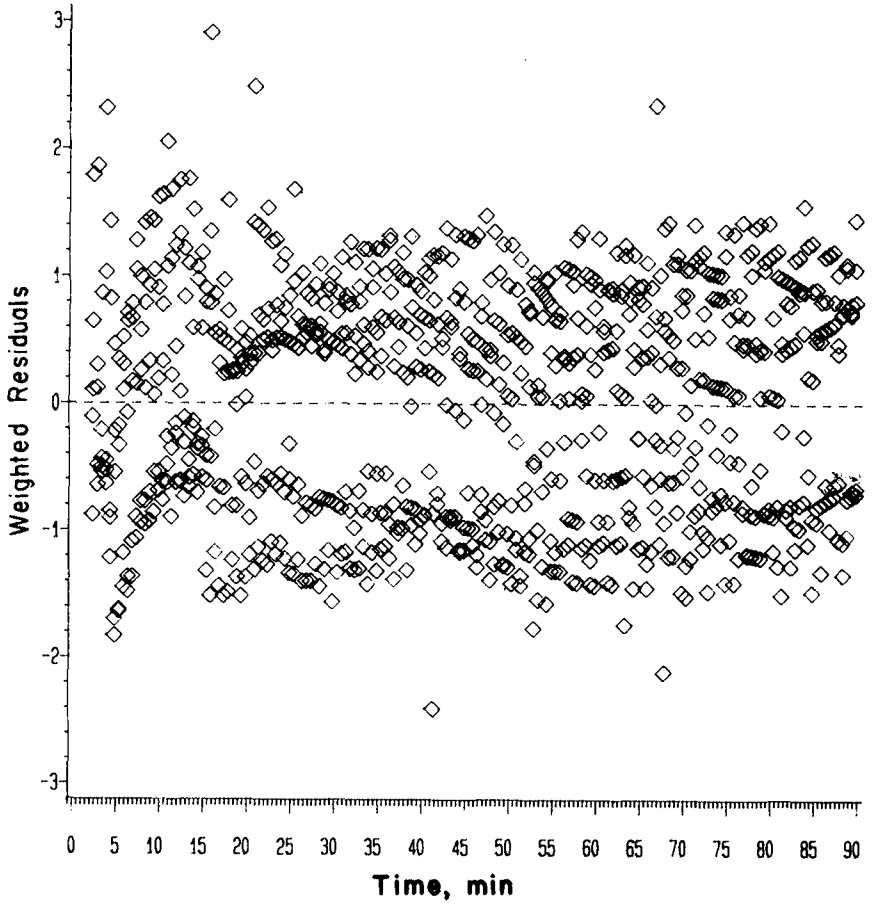


Fig. 4. Residuals weighted by pure error variances from five replicate runs for the multisite model.

When the multisite model was fitted to the data from these runs, the residuals plot, shown in Figure 3 was obtained. It is clearly visible that the pure error variance is not constant with polymerization time; there is a significant decrease in pure error variance as polymerization proceeds. This phenomenon may result from many causes: (i) the kinetic curve is much steeper at early times, which results in larger errors in monomer feed rate measurements; (ii) the transient behavior of monomer concentration is greater during the early stages of polymerization; hence gas-absorption corrections become more significant; and (iii) the catalyst may disintegrate into separate particles at slightly different rates from run to run, which makes the kinetic data at early times less reliable.

TABLE I
Correlation Matrix for Parameters Obtained Using Weighted Least-Squares for Five Replicate Runs

| | $\theta_1$ | $\theta_2$ | $\theta_3$ |
|---|---|---|---|
| $\theta_1$ | 1.000 | 0.965 | 0.810 |
| $\theta_2$ | — | 1.000 | 0.933 |
| $\theta_3$ | — | — | 1.000 |

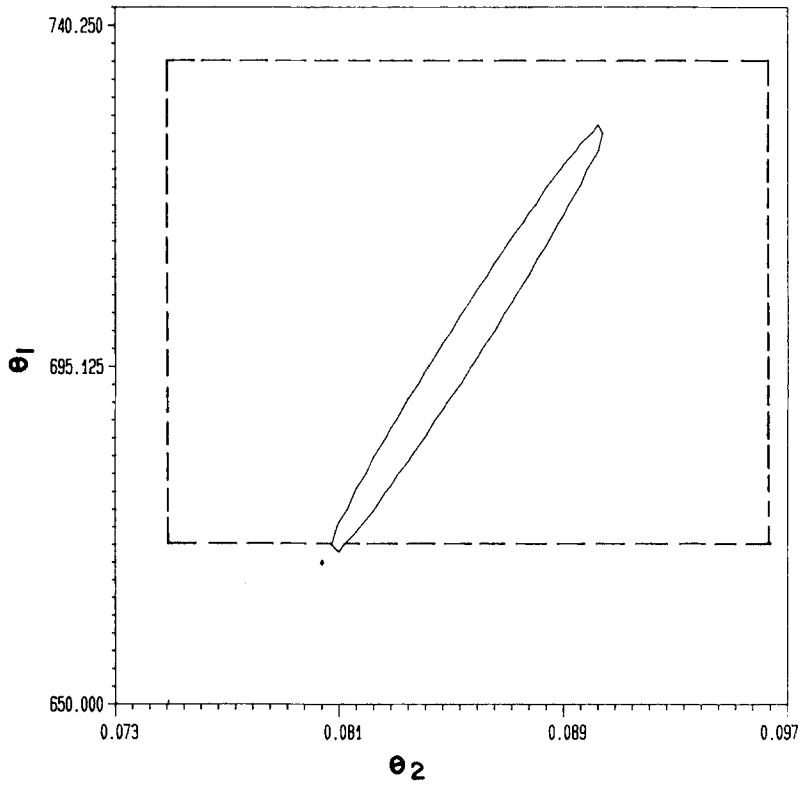


Fig. 5. Joint confidence region for $\theta_1$ and $\theta_2$ at $\theta_3 = 1.16$. The dotted box encloses the 95% joint confidence intervals, and the solid figure encloses the 95% joint confidence region.

Of course nonconstant variance, as observed in Figure 3, violates one of the basic assumptions of least squares regression. Therefore, the model was refitted with each data point weighted inversely proportional to its pure error variance. The residuals plot obtained using weighted least squares is shown in Figure 4. Here, the variance is relatively constant as a function of polymerization time, and there do not appear to be any trends which might indicate model inadequacy. Quantitative assessments of model adequacy could not be applied in this case because a pooled estimate of the pure error variance could not be obtained.

Because it would be excessively time-consuming to obtain such a large number of replicates for each set of operating conditions being investigated, the set of weights computed from these replicates was also employed for all the other runs in parameter estimation.

For those five replicate runs the correlation matrix for the parameter estimates obtained using weighted least squares is given in Table I, showing moderate correlation. High correlations between parameters and intrinsic nonlinearity can distort the shapes of joint confidence regions and make parameter estimates unreliable (Pritchard and Bacon[10]).

It is difficult to appreciate the effect of correlation on a joint confidence region by a numerical value alone. Therefore, true joint confidence regions for

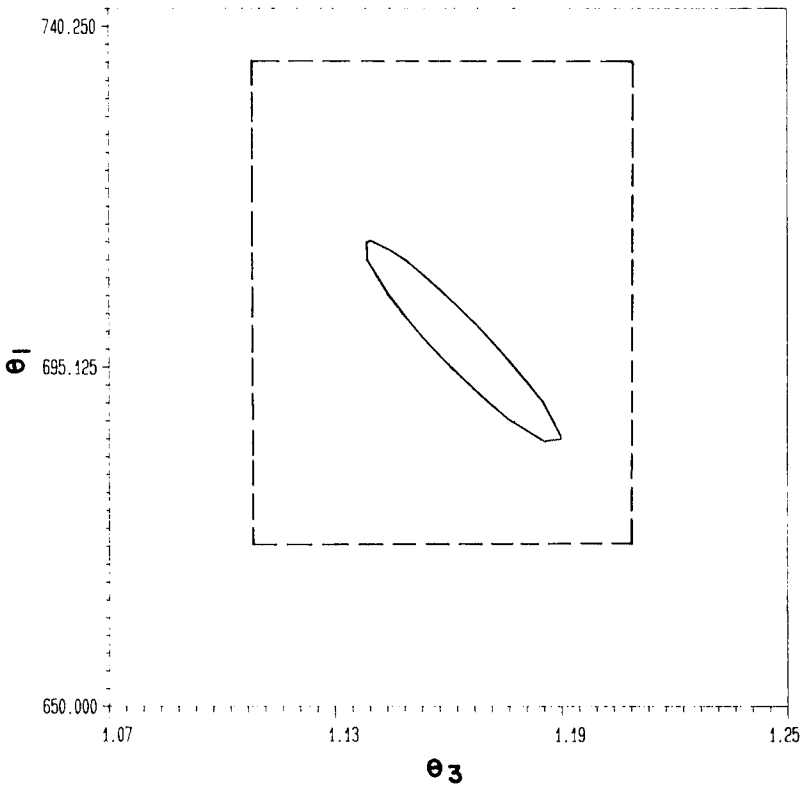


Fig. 6. Joint confidence region for $\theta_1$ and $\theta_3$ at $\theta_2 = 0.09$. The dotted box encloses the 95% joint confidence intervals, and the solid figure encloses the 95 joint confidence region.

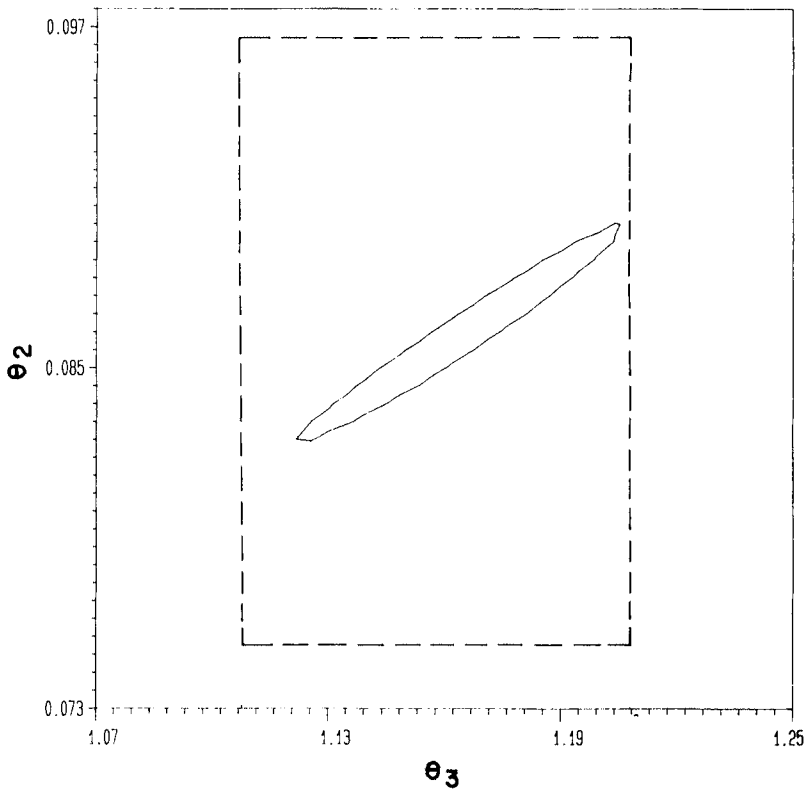


Fig. 7. Joint confidence region for $\theta_2$ and $\theta_3$ at $\theta_1 = 698.0$. The dotted box encloses the 95% joint confidence intervals, and the solid figure encloses the 95% joint confidence region.

parameters $\theta_1 - \theta_2$, $\theta_1 - \theta_3$, and $\theta_2 - \theta_3$ were mapped out in Figures 5–7, respectively. These 95% joint confidence intervals were computed using the relationship (Draper and Smith[11]):

$$S(\theta) \leq \hat{S}(\theta)\{1 + p/(n-p)F_{p,n-p,1-\alpha}\} \tag{12}$$

where $S(\theta)$ = sum of squares of residuals, $\hat{S}(\theta)$ = minimum value of S($\theta$), $p$ = number of parameters, $n$ = number of data points, and $\alpha$ = confidence level parameter. The joint confidence region obtained in this manner is exact; however, the confidence level (95%) is approximate. Also, superimposed onto these plots is the confidence region estimated using "NOTLIN" based on a linearization method. Comparison of the joint confidence regions obtained by these two methods indicates that the correlation between parameters and intrinsic nonlinearity do not significantly inflate the variance associated with parameter estimates. The confidence intervals predicted using "NOTLIN" enclosed the true joint confidence region in all cases. Qualitatively, the true joint confidence regions of Figures 5–7 indicate a very low degree of intrinsic nonlinearity, because they are very elliptical in shape, rather than banana-shaped or otherwise distorted in shape, as is the case with high intrinsic nonlinearity (Box and Draper[12]).

TABLE II
Summary of Experimental Conditions and Parameter Estimates[a]

| Expt no | Cat. batch | $T$ (°C) | Ti ($\mu$ mol) | Al/Ti | TMPIP/Ti | $\theta_1$, (L/min mol Ti) | $\theta_2$ 1/min | $\theta_3$ |
|---|---|---|---|---|---|---|---|---|
| 63 | 3 | 50 | 64.4 | 21.3 | 0 | 550 (38) | 0.13 (0.02) | 1.44 (0.04) |
| 64 | 3 | 50 | 65.3 | 32.0 | 0 | 636 (35) | 0.09 (0.01) | 1.06 (0.06) |
| 65 | 3 | 50 | 64.5 | 42.5 | 0 | 788 (56) | 0.25 (0.03) | 1.14 (0.03) |
| 66 | 3 | 50 | 62.1 | 52.9 | 0 | 838 (54) | 0.23 (0.02) | 1.17 (0.03) |
| 67 | 3 | 50 | 63.3 | 62.0 | 0 | 1281 (222) | 0.55 (0.15) | 1.22 (0.03) |
| 68 | 3 | 50 | 61.9 | 10.8 | 0 | 447 (12) | 0.034 (0.003) | 1.24 (0.12) |
| 71 | 3 | 50 | 63.8 | 25.5 | 0 | 753 (40) | 0.13 (0.01) | 1.10 (0.04) |
| 72 | 3 | 50 | 61.8 | 74.4 | 0 | 1371 (222) | 0.56 (0.15) | 1.25 (0.03) |
| 73 | 3 | 50 | 61.8 | 15.5 | 0 | 390 (10) | 0.024 (0.003) | 1.35 (0.18) |
| 76 | 3 | 50 | 63.0 | 15.2 | 0 | 644 (28) | 0.04 (0.006) | 1.33 (0.16) |
| 77 | 3 | 50 | 62.9 | 36.6 | 0 | 929 (48) | 0.20 (0.02) | 1.12 (0.02) |
| 78 | 3 | 50 | 63.3 | 25.7 | 0 | 872 (42) | 0.098 (0.001) | 1.02 (0.04) |
| 79 | 3 | 50 | 64.3 | 4.9 | 0 | 167 (6) | 0.115 (0.004) | 0.00042 (0.00001) |
| 80 | 3 | 50 | 62.4 | 10.7 | 0 | 505 (14) | 0.024 (0.001) | 0.057 (0.007) |
| 81 | 3 | 50 | 62.7 | 84.0 | 0 | 1391 (130) | 0.78 (0.12) | 1.27 (0.02) |
| 84 | 3 | 50 | 62.6 | 18.1 | 0 | 640 (36) | 0.091 (0.012) | 1.24 (0.04) |
| 85 | 3 | 50 | 65.2 | 5.1 | 0 | 249 (14) | 0.115 (0.006) | 0.00109 (0.00006) |
| 89 | 3 | 50 | 87.2 | 16.1 | 0 | 628 (37) | 0.064 (0.012) | 1.31 (0.12) |
| 92 | 3 | 50 | 153.0 | 6.5 | 0 | 569 (24) | 0.026 (0.002) | − 0.0049 (0.002) |
| 93 | 3 | 50 | 129.0 | 5.8 | 0 | 599 (22) | 0.046 (0.003) | 0.40 (0.04) |
| 94 | 3 | 50 | 114.0 | 6.1 | 0 | 549 (14) | 0.037 (0.002) | 0.24 (0.03) |
| 95 | 3 | 50 | 95.5 | 6.3 | 0 | 346 (10) | 0.039 (0.002) | 0.22 (0.03) |
| 96 | 3 | 50 | 47.2 | 30.7 | 0 | 825 (74) | 0.14 (0.03) | 1.23 (0.08) |
| 98 | 3 | 50 | 53.6 | 55.0 | 0 | 1027 (38) | 0.27 (0.02) | 1.19 (0.02) |
| 107 | 4 | 50 | 41.4 | 24.2 | 0 | 1230 (172) | 0.22 (0.08) | 1.83 (0.14) |
| 108 | 4 | 50 | 41.4 | 24.2 | 0 | 1537 (120) | 0.19 (0.04) | 1.27 (0.06) |
| 111 | 4 | 50 | 41.4 | 24.2 | 0 | 1171 (110) | 0.19 (0.04) | 1.53 (0.06) |
| 112 | 4 | 50 | 41.4 | 24.2 | 0 | 1515 (208) | 0.25 (0.07) | 1.37 (0.07) |
| 114 | 4 | 55 | 41.4 | 24.2 | 0 | 1187 (137) | 0.25 (0.07 | 1.82 (0.08) |
| 116 | 4 | 55 | 41.4 | 24.2 | 0 | 1405 (86) | 0.25 (0.05) | 1.78 (0.08) |
| 117 | 4 | 55 | 41.4 | 24.2 | 0 | 1490 (121) | 0.36 (0.08) | 1.96 (0.05) |
| 120 | 4 | 60 | 41.4 | 24.2 | 0 | 1602 (96) | 0.60 (0.10) | 1.81 (0.06) |
| 125 | 4 | 40 | 41.4 | 24.2 | 0 | 273 (10) | 0.019 (0.003) | 1.41 (0.31) |
| 126 | 4 | 40 | 41.4 | 24.2 | 0 | 362 (10) | 0.0153 (0.0006) | 0.039 (0.004) |
| 129 | 4 | 30 | 62.1 | 24.2 | 0 | 137 (2) | 0.0121 (0.0004) | 0.10 (0.01) |
| 133 | 4 | 30 | 62.1 | 24.2 | 0 | 272 (16) | 0.036 (0.007) | 1.39 (0.22) |
| 136 | 4 | 20 | 82.7 | 24.2 | 0 | 80 (2) | 0.014 (0.001) | 0.35 (0.19) |
| 165 | 5 | 50 | 53.9 | 55.7 | 0 | 881 (75) | 0.23 (0.04) | 1.23 (0.06) |
| 166 | 5 | 50 | 53.9 | 55.7 | 0 | 907 (75) | 0.25 (0.06) | 1.19 (0.11) |
| 167 | 5 | 50 | 53.9 | 55.7 | 5.5 | 790 (73) | 0.23 (0.06) | 1.39 (0.11) |
| 168 | 5 | 50 | 53.9 | 55.7 | 27.5 | 576 (24) | 0.10 (0.01) | 1.13 (0.07) |
| 169 | 5 | 50 | 53.9 | 55.7 | 27.5 | 643 (44) | 0.15 (0.02) | 1.49 (0.11) |
| 170 | 5 | 50 | 53.9 | 55.7 | 49.5 | 389 (26) | 0.07 (0.01) | 1.16 (0.11) |
| 171 | 5 | 50 | 53.9 | 55.7 | 49.5 | 684 (101) | 0.13 (0.04) | 1.15 (0.13) |
| 173 | 5 | 50 | 53.9 | 55.7 | 49.5 | 282 (17) | 0.07 (0.01) | 1.16 (0.11) |

[a] Experiments were performed at 1.18 ± .01 bar; Al/Ti and TMPIP/Ti are expressed as molar ratio; and $\theta_1 V \Sigma p_i [C_i^*]$, where $V$ is the reaction mixture volume, 0.23 L, and the values in parenthesis under $\theta$ are standard deviations.

## Effects of Operating Conditions and Additives on Parameters $\theta_1$, $\theta_2$, and $\theta_3$

The reactor system, experimental procedures for catalyst preparation, polymerization, and mass transfer correction to obtain true rate data have been discussed in Part I of this series.[7]

Experiments were carried out to determine the effects of certain operating variables such as Al/Ti ratio, temperature, and 2, 2, 6, 6-tetramethylpiperidine (TMPIP) concentration on polymerization. By subsequently fitting the multisite kinetic model to the data, relationships between these operating variables and kinetic parameters were obtained. These results were then interpreted in an effort to further understand the fundamentals of this polymerization system. The detailed experimental conditions and the associated parameter estimates are tabulated in Table II.

### *Al / Ti Ratio*

The effect of Al/Ti ratio on the multisite kinetic model parameters $\theta_1$, $\theta_2$, and $\theta_3$ are shown in Figures 8, 9, 10, respectively. Figure 8 shows that $\theta_1$

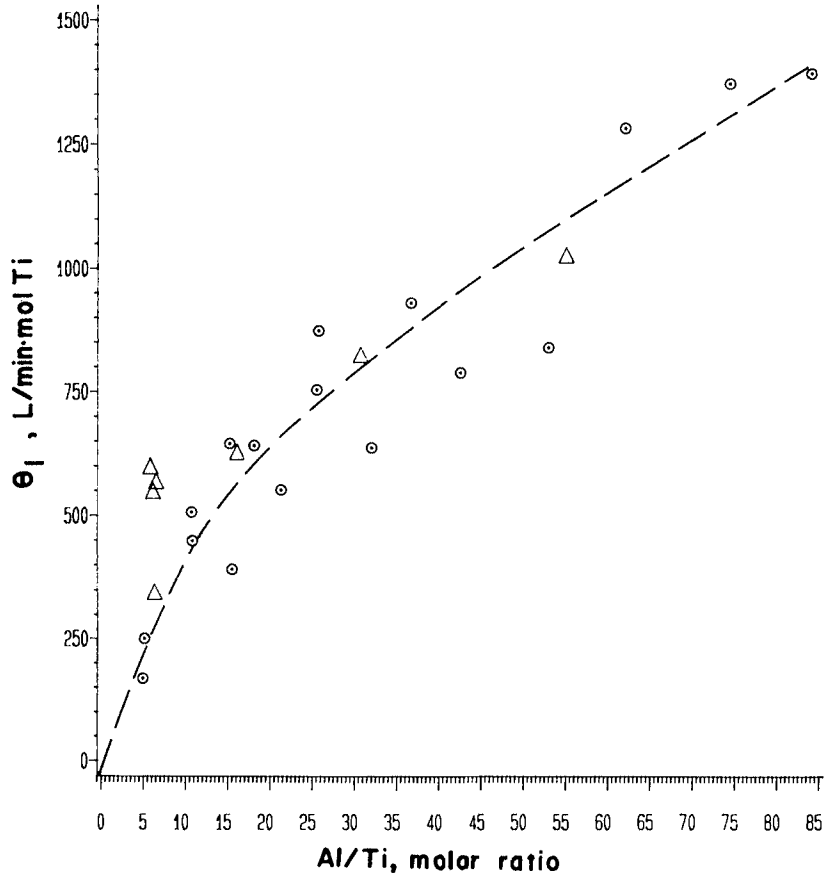


Fig. 8. Effect of Al/Ti on $\theta_1$ at 50°C: (⊙) runs performed using 40 mg of catalyst; (△) runs performed using 29–94 mg of catalyst. The reaction mixture volume is 0.23 L.

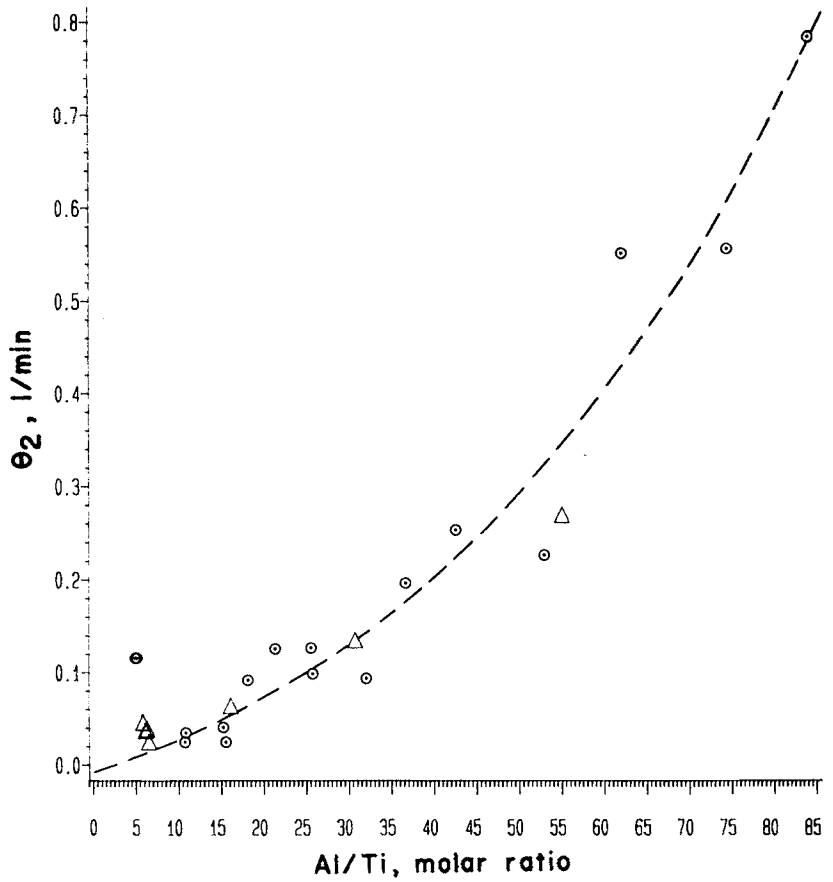


Fig. 9. Effect of Al/Ti on $\theta_2$ at 50°C: (⊙) runs performed using 40 mg of catalyst; (△) runs using 29–94 mg of catalyst.

increases continuously as the Al/Ti ratio increases; no optimum exists. Figure 9 indicates that $\theta_2$ also increases continuously with Al/Ti ratio. The combined effect of Al/Ti on $\theta_1$ and $\theta_2$ results in the optimum productivity discussed in Part I of this study.[7] This explains why an optimum in productivity is not observed at early polymerization times, because a large number of sites have not been terminated during the first 5 min. Comparison of Figures 8 and 9 indicates that sites with higher activities also decay at higher rates. As discussed previously by Dumas and Hsu[3], this is in agreement with results obtained by Giannini[9] and Doi et al.[8] through CO quenching of active sites.

The effect of Al/Ti ratio on the heterogeneity parameter $\theta_3$ is shown in Figure 10. It is clear that, at low Al/Ti ratios $\theta_3$ approaches zero and as Al/Ti increases to approximately 15, $\theta_3$ increases rapidly to approximately 1.3. Beyond this point, $\theta_3$ remains relatively constant, and, although certain trends reflecting changes in heterogeneity may actually exist, they are difficult to identify because of the large degree of scatter and because $\theta_3$ is correlated to a certain extent with $\theta_1$ and $\theta_2$. Interpretation of these results, in light of the model simulations, suggests that the system becomes more homogeneous

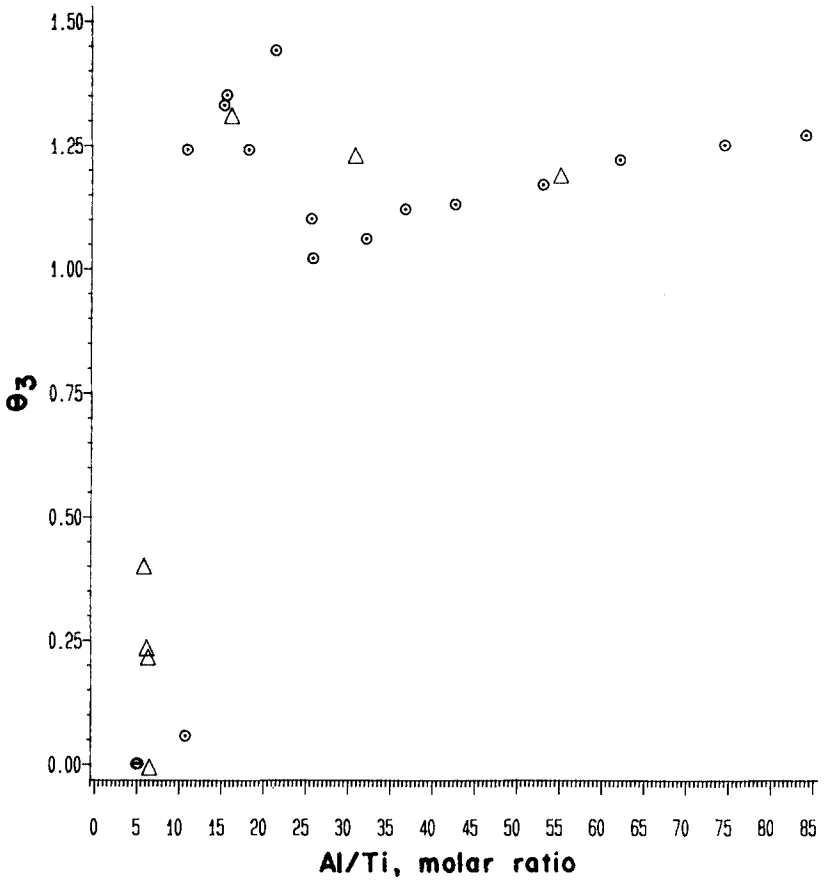


Fig. 10. Effect of Al/Ti on $\theta_3$ at 50°C: (⊙) runs performed using 40 mg of catalyst; (△) runs performed using 29–94 mg of catalyst.

in activity as the Al/Ti ratio becomes small. If the system was in fact homogeneous, the single-site kinetic model would provide as good a fit to the experimental data as the multisite model. Therefore, to test this, the single-site model was also fitted to a variety of runs. The adequacy of multiple-site and single-site models was compared using weighted sum of squares of residuals values (Table III). Clearly, at low Al/Ti ratios the single-site model provides as good a fit as the multisite model. However, as the Al/Ti ratio increases beyond approximately 6, the single-site model becomes inadequate.

Furthermore, the effect of Al/Ti ratio on the isotactic index also supports this conclusion. There are sites that are isotactic-specific while others are atactic-specific. As shown in Part I (Dumas and Hsu[7]), tacticity increases with decreasing Al/Ti ratio. Perhaps, as the Al/Ti ratio increases, the heterogeneity in sites also increases and a larger fraction of atactic-specific sites are created.

### *Temperature*

In Part I, an optimum in productivity with polymerization temperature was observed. With the aid of the multisite kinetic model, this can be explained in

TABLE III
Comparison of Weighted Sums of Squares of Residuals Using Multisite and Single-Site Models for Runs Performed with Various Al/Ti Ratios

| Run no. | Al/Ti molar ratio | Weighted sum of squares of residuals for the multisite model | Weighted sum of squares of residuals for the single-site model |
|---|---|---|---|
| 79 | 4.9 | 0.6 | 0.6 |
| 85 | 5.1 | 72 | 73 |
| 94 | 6.1 | 39 | 80 |
| 83 | 8.3 | 15 | 67 |
| 68 | 10.8 | 12 | 100 |
| 89 | 16.1 | 35 | 304 |
| 63 | 21.3 | 11 | 144 |
| 71 | 25.5 | 11 | 141 |

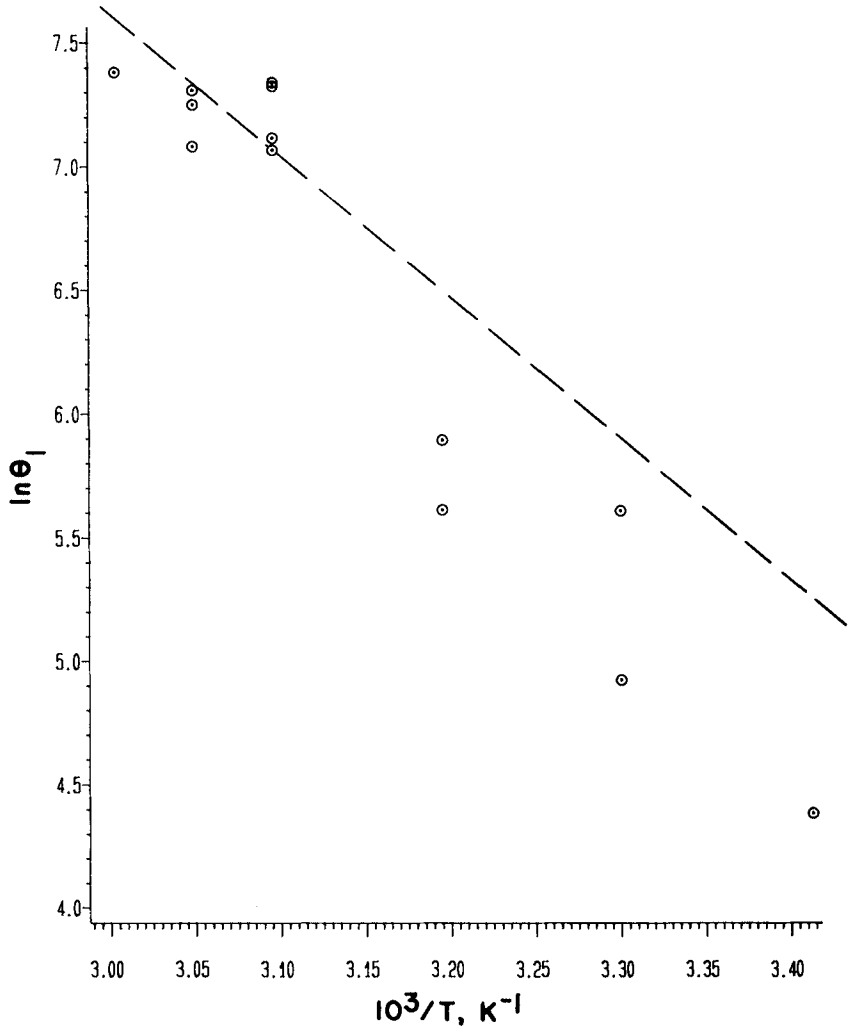


Fig. 11. Arrhenius plot for $\theta_1$ at Al/Ti = 25. The line was obtained by fitting the Arrhenius expression in its nonlinear form to the data.

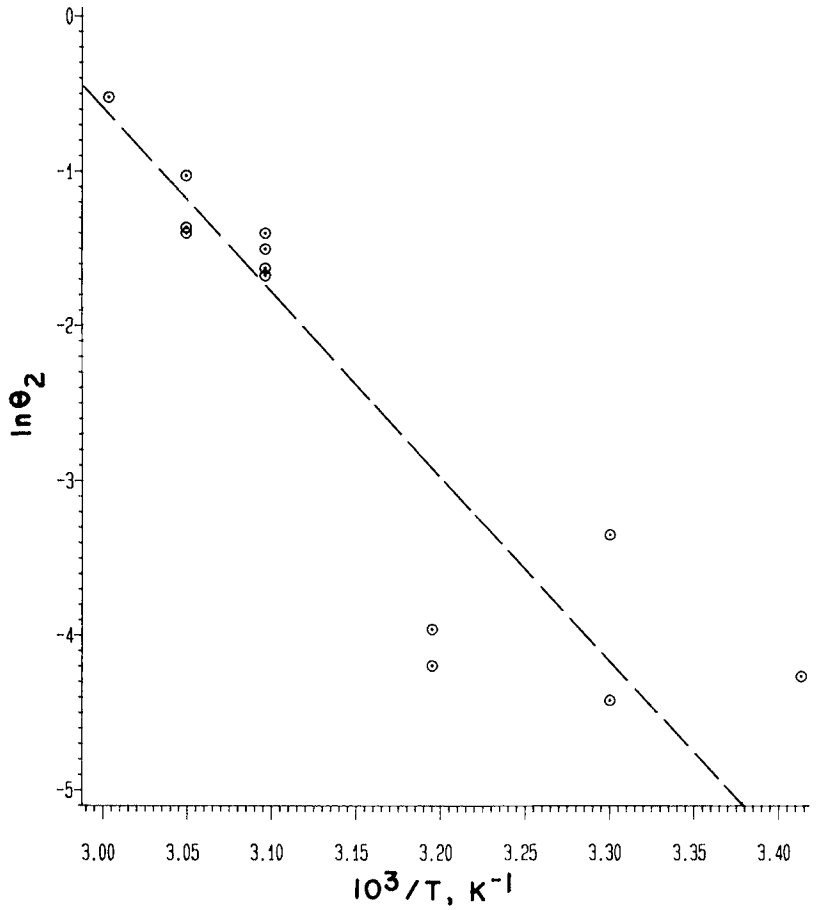


Fig. 12. Arrhenius plot for $\theta_2$ at Al/Ti = 25. The line was obtained by fitting the Arrhenius expression in its nonlinear form to the data.

a similar manner as discussed in the previous section. Figure 11 shows an Arrhenius-type plot for $\theta_1$. Clearly, $\theta_1$ increased with polymerization temperature; no optimum behavior is observed. The Arrhenius-type plot for $\theta_2$ (Fig. 12) indicates that $\theta_2$ also increases monotonically with temperature. Therefore, as activity and termination both increase with temperature, at differing rates, an optimum in productivity should be observed.

The effect of temperature on $\theta_3$ (Fig. 13) is difficult to determine because of scatter in the data. However, in general, $\theta_3$ increases with polymerization temperature. Because $\theta_3$ reflects heterogeneity of sites, this may explain the increase in tacticity with temperature. As has already been discussed by Dumas and Hsu,[3] an increase in the composition of isotactic polypropylene with increasing polymerization temperature is commonly observed. Perhaps it can be explained that an increase in the heterogeneity of sites with temperature will result in an increase in the fraction of isotactic-specific sites.

### *Addition of 2, 2, 6, 6-tetramethylpiperidine*

As already discussed in Part I of this series,[7] TMPIP improves tacticity by blocking atactic-specific sites; and when isotactic specific sites are also blocked,

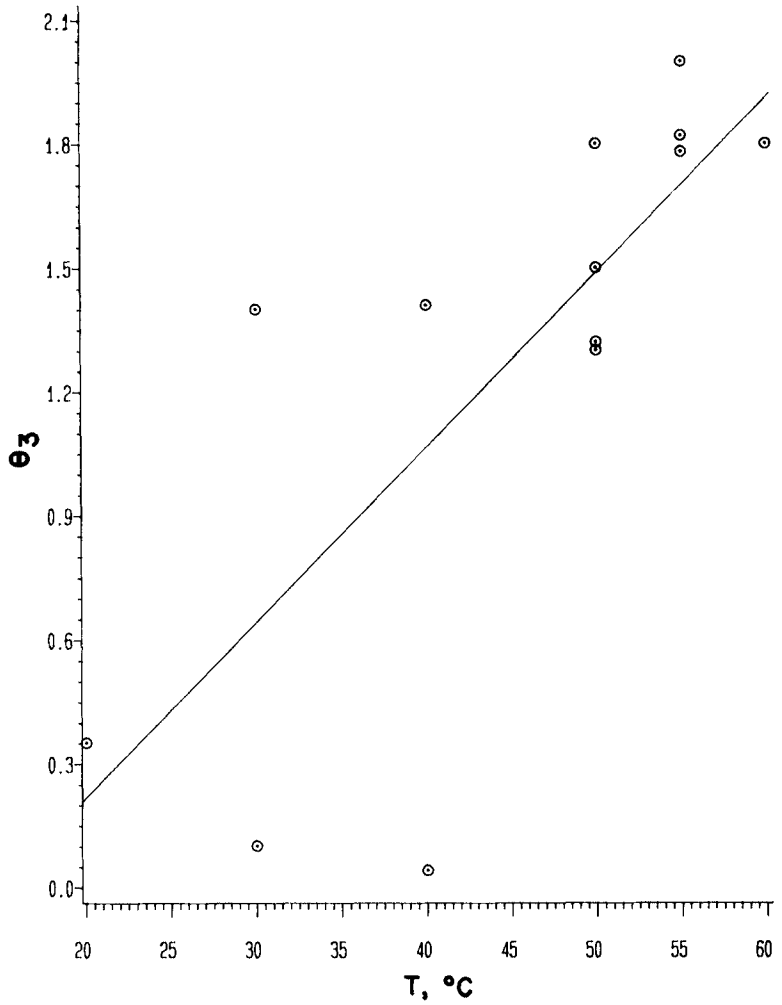


Fig. 13. Effect of temperature on $\theta_3$ at Al/Ti = 25.

a significant reduction in productivity would be observed. This relation was not what we observed in this work. The productivity is only slightly decreased with the addition of TMPIP. This can be explained by examining the effect of TMPIP on the kinetic parameters.

As shown in Figure 14, addition of TMPIP resulted in a decrease in $\theta_1$, or activity. Termination, or $\theta_2$, also decreased with added TMPIP (Fig. 15). Doi et al.[8] observed that when sites were poisoned by CO, the more active variety of sites were preferentially destroyed. Therefore, it could be suggested that TMPIP reduces activity, by poisoning sites in such a manner that the more active sites are preferentially poisoned. Also because the more active sites also terminate faster, the net effect is a decrease in the overall termination rate. The compensation effect leads to only a slight decrease in productivity.

Unfortunately, the scatter in the $\theta_3$ data, Figure 13, makes it difficult to draw conclusions concerning the effect of TMPIP on the heterogeneity parameter.

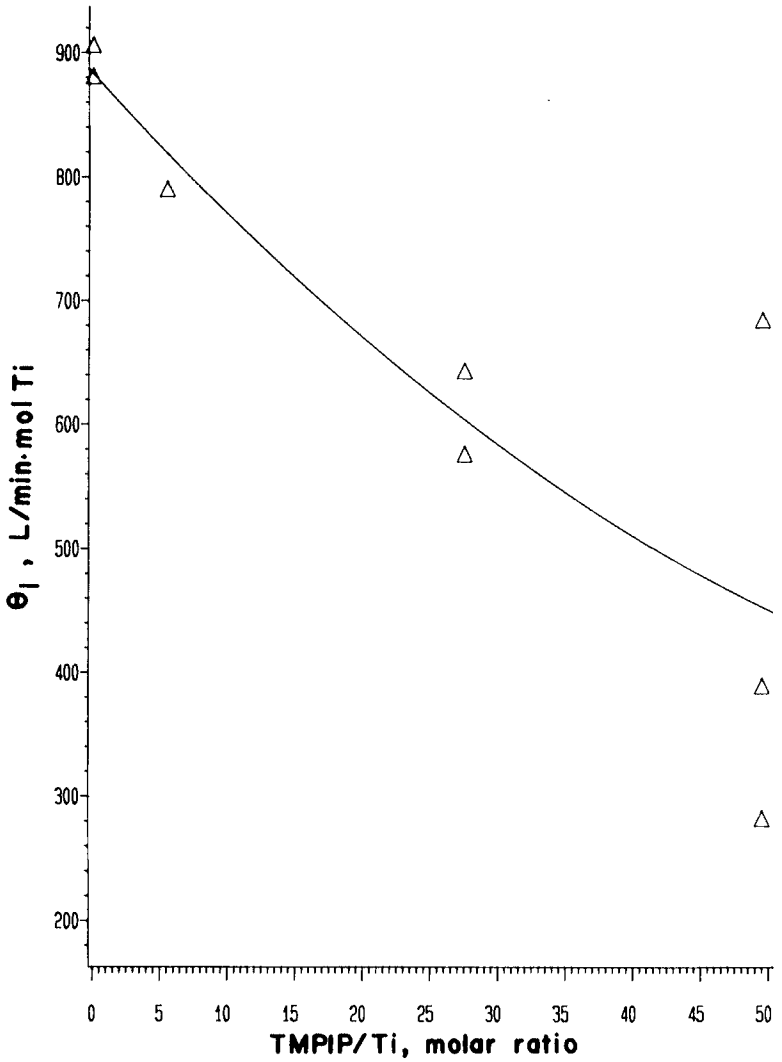


Fig. 14. Effect of 2, 2, 6, 6-tetramethylpiperidine on $\theta_1$ at 50° C and Al/Ti = 50.

## CONCLUSIONS

A mechanistic kinetic model was developed that could account for the possible existence of a variety of active sites with different polymerization characteristics. By fitting the multisite model to these simulated data obtained for various types of sites distributions, it was shown that the power law approximation was valid for a variety of distributions of active sites.

A large number of replicate runs performed at 50°C and at Al/Ti ratio of 21 allowed a detailed statistical investigation of the multisite model which indicated the following: that (i) the experimental data were heteroscedastic, and therefore weighted least squares had to be performed to obtain unbiased parameter estimates; that (ii) the nature of the shapes of the true joint

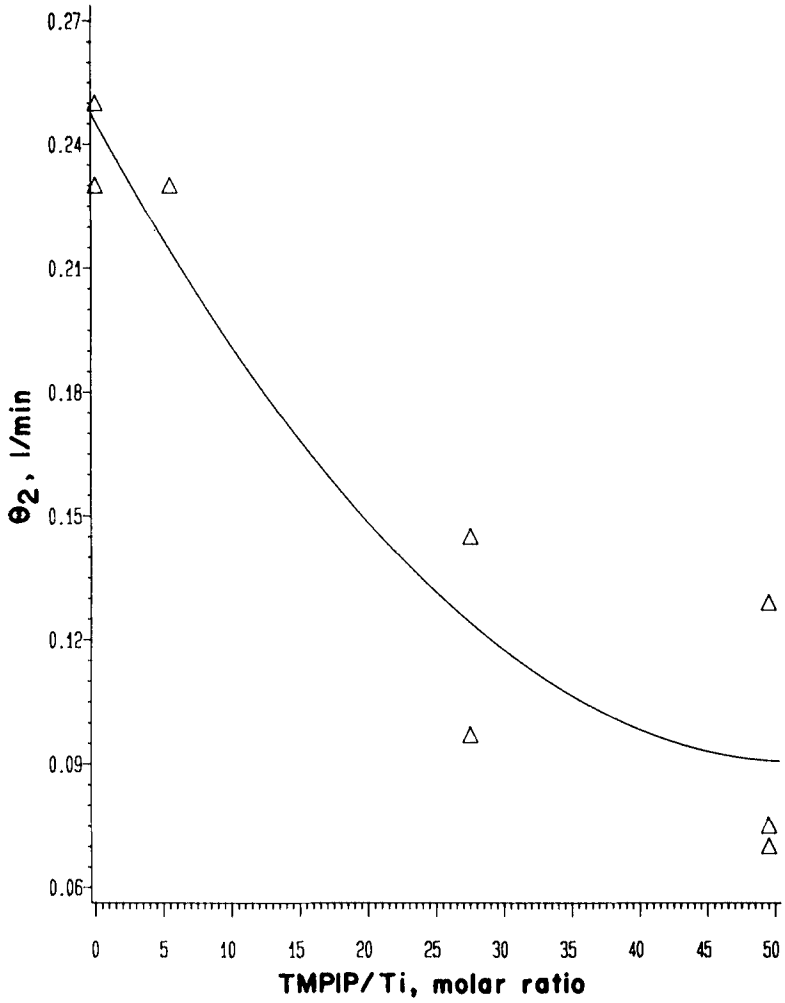


Fig. 15. Effect of 2, 2, 6, 6-tetramethylpiperidine on $\theta_2$ at 50 °C and Al/Ti = 50.

confidence regions indicated that the model exhibited a relatively low degree of intrinsic nonlinearity; that (iii) the correlations between parameters did not unduly inflate the precision associated with parameter estimates; and that (iv) the model gave a good description of this polymerization system consisting of a variety of active sites. There were no visible trends in the residuals which might indicate model inadequacy, whereas the single-site model was clearly inadequate.

Kinetic modeling of experimental data obtained under various operating conditions has enabled us to make the following conclusions:

i. As the Al/Ti ratio becomes small (Al/Ti < 6), the system becomes more homogeneous in the distribution of active sites.

ii. Although an optimum in productivity was observed at an Al/Ti ratio of approximately 15, fitting of the multisite model to the data indicated that both activity and termination terms increased continuously with Al/Ti ratio,

but at different rates, and the combined effect resulted in an optimum in productivity.

iii. The multisite model also shows that both activity and termination terms increase, at different rates, with polymerization temperature. This explains the optimum in productivity with respect to temperature.

iv. The improved tacticity with the use of TMPIP can be explained by selectively poisoning atactic-specific sites. When sites are poisoned, the sites which normally deactivate at a higher rate are preferentially poisoned first.

Financial support for this work was provided by the Natural Sciences and Engineering Research Council Of Canada.

## References

1. T. Keii, E. Suzuki, M. Tamura, M. Murata, and Y. Doi, *Makromol. Chem.*, **183**, 2285 (1982).
2. N. F. Brockmeier and J. B. Rogan, *AIChE Mtg. Anaheim, CA (May)*, (1984).
3. C. Dumas and C. C. Hsu, *J. Macromol. Sci., Rev. Macromol. Chem. Phys.*, **24**, 1355 (1984).
4. J. C. W. Chien and J.-C. Wu, *J. Polym. Sci., Polym, Chem. Ed.*, **20**, 2461 (1982).
5. J. C. W. Chien and C.-I. Kuo, *J. Polym. Sci., Polym. Chem. Ed.*, **23**, 731 (1985).
6. R. R. D. Kemp and B. W. Wojciechowski, *Ind. Eng. Chem. Fundam.*, **13**, 332 (1974).
7. C. Dumas and C. C. Hsu, *J. Appl. Polym. Sci.*, to appear.
8. Y. Doi, M. Murata, and K. Yano, *Ind. Eng. Chem., Prod. Res. Dev.*, **21**, 580 (1982).
9. U. Giannini, *Makromol. Chem. Suppl.*, **5**, 216 (1981).
10. D. J. Pritchard and D. W. Bacon, *Chem. Eng. Sci.*, **33**, 1539 (1978).
11. N. R. Draper and H. Smith, *Applied Regression Analysis*, 2nd ed., Wiley, New York, 1981.
12. G. E. Box and N. R. Draper, *Biometrika*, **52**, 355 (1965).

Received March 3, 1986
Accepted January 8, 1988